Vision Research 161 (2019) 52–59

Contents lists available at ScienceDirect

Vision Research

journal homepage: www.elsevier.com/locate/visres

Effect of high-order aberrations on pattern-reversal visual evoked potentials

Yan-rong Yang[a,1], Jun-lei Zhao[b,c,*,1], Fei Xiao[b,c], Hao-xin Zhao[b,c], Yun Dai[b,c,*]

[a] College of Ophthalmology, Chengdu University of Traditional Chinese Medicine, Chengdu 610075, China
[b] Chinese Academy of Sciences, The Key Laboratory of Adaptive Optics, No.1 Guangdian Avenue Xihang Port Shuangliu, Chengdu 610209, China
[c] Chinese Academy of Sciences, Institute of Optics and Electronics, No.1 Guangdian Avenue Xihang Port Shuangliu, Chengdu 610209, China

ARTICLE INFO

Keywords:
Ophthalmic optics and devices
Active or adaptive optics
Visual evoked potential
High-order aberrations

ABSTRACT

To investigate the effect of high-order aberrations (HOAs) on pattern-reversal visual evoked potentials (PR-VEPs), we measured PR-VEPs with HOAs either retained or corrected with an adaptive optics (AO) system for 12 subjects. The PR-VEPs at different spatial frequencies were recorded for the dominant eye of each subject. The results indicated that the amplitude of the first positive P1 wave at 1–16 cpd (except 2 cpd) and the second negative N2 wave at 12 and 16 cpd were raised statistically significantly with HOA correction. This confirmed the contributions of the HOAs to the alterations in PR-VEPs, and suggested that HOAs should be corrected to realize accurate PR-VEP testing.

1. Introduction

The visual evoked potential (VEP) is a minute neural discharge that occurs in the human visual cortex in response to patterns or other stimulation of the retina. After the retina receives a pattern stimulus, the generated signal passes through the visual pathway to the visual cortex, where the summed electrical activity is termed the evoked potential. A VEP is recorded using scalp electrodes, through amplification and summation, and it produces a characteristic waveform with a negative-positive-negative (NPN) wave (Odom et al., 2010). The amplitude of the NPN wave reflects the number of nerve fibers that reach the visual cortex, while the latency reflects the functional integrity of the myelin along the visual pathway and the different transmission channels. As such, the NPN wave serves as a sensitive indicator of a variety of pathological conditions, such as amblyopia, (Gundogan et al., 2010; Wenner et al., 2014) glaucoma, (Abe, Hasegawa, & Iwata, 1987) optic neuritis, (Halliday, McDonald, & Mushin, 1972) multiple sclerosis, (Hoeppner & Lolas, 1978) and other visual pathway dysfunctions originating from the receptor cells to the visual cortex. These pathological conditions can change the amplitude or latency of the VEP or both.

However, many non-pathological factors may affect VEP testing (Andreassi et al., 1970; Dion et al., 2013; Stockard et al., 1979; Halliday, 1982; Abdullah et al., 2012). Among these factors, ocular aberration is one of the most important influential factors (Bach & Mathieu, 2004; Mezer et al., 2004) because it directly degrades the retinal image quality of the pattern stimulus, and may affect all pattern-based electrophysiological responses, such as the pattern visual evoked potential (PVEP) and pattern electro-retinograms (PERGs). At present, for refraction errors or eye aberrations, wearing glasses corrects only defocus and astigmatism in PVEP testing. A number of studies have been conducted to examine the effect of defocusing on PVEP. In Harter and White (1968) first studied the influence of the outline sharpness of an image on the PVEP. They pointed out that the amplitude of the PVEP was reduced when retinal imaging was degraded by dioptric defocus simulated by plus lenses. Based on this relationship, the defocus, astigmatism, and astigmatism axes can be measured quickly and objectively using the PVEP (Regan, 1973). In addition to reducing the pattern-reversal visual evoked potential (PR-VEP) amplitude, the introduced defocus prolongs the P100 latency (Collins, Carroll, Black, & Walsh, 1979). Thus, upon decreasing the visual acuity using a positive lens, the PVEP latency falls outside the normal range (Bartel & Vos, 1994). Thus, when using VEPs for visual pathway disease diagnosis and other clinical examinations, refractive errors must be corrected to avoid their effect on diagnosis. In Kothari, Bokariya, Singh, Narang, and Singh (2014) made a comprehensive summary of the impact of refractive errors on VEPs.

It is well known that the human eye suffers from high-order aberrations (HOAs) in addition to defocus and astigmatism (which are low-order aberrations, or LOAs), which also greatly degrade retinal image quality (Liang, Grimm, Goelz, & Bille, 1994). The effects of HOAs on

* Corresponding authors at: Chinese Academy of Sciences, The Key Laboratory of Adaptive Optics, No.1 Guangdian Avenue Xihang Port Shuangliu, Chengdu 610209, China.
E-mail addresses: hustoejunzuo@163.com (J.-l. Zhao), daiyunqq@163.com (Y. Dai).
[1] These authors contributed equally to this work, and should be considered co-first authors.

https://doi.org/10.1016/j.visres.2019.05.008
Received 6 December 2018; Received in revised form 18 April 2019; Accepted 17 May 2019
Available online 26 June 2019
0042-6989/

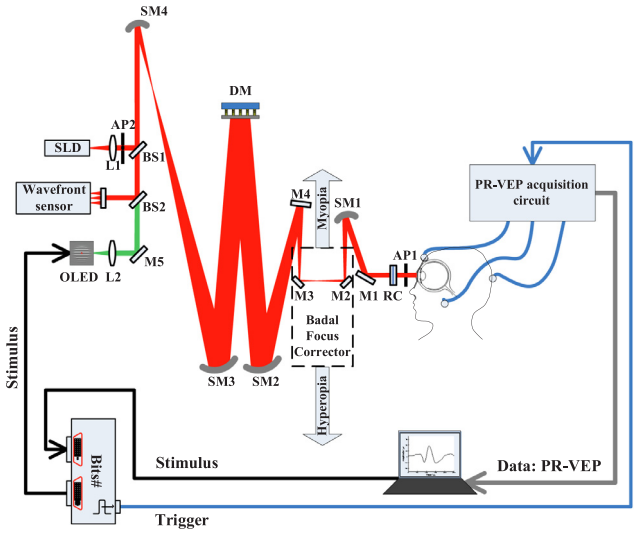

Fig. 1. Schematic of AO PR-VEP measurement system. SLD, super-luminescent diode; SM, spherical mirror, BS, beam splitter; M, mirror; DM, 145-element PZT deformable mirror; L, lens; AP1, artificial exit pupil; AP2, artificial entrance pupil; RC, rotating cylinders, OLED, organic light-emitting-diode.

visual function should not simply be neglected, as suggested by some vision researchers and neurophysiologists (Williams et al., 1997; Roorda, 2011). While it is worth researching whether the HOAs remain important for VEP testing, no relevant studies have been reported until now, which prompted us to conduct the research reported in this paper.

In this article, we investigate the effects of HOAs on PR-VEPs. PR-VEP measurements of 12 subjects with normal vision were performed with HOAs that were either retained or corrected by an AO system. The influence of HOAs on each component of the PR-VEP was analyzed.

2. Methods

2.1. Apparatus

In this study, an AO PR-VEP measurement system was used as the experimental platform (Yang et al., 2018). Fig. 1 is a schematic of the experimental system, which consisted of an adaptive optics (AO) and a PR-VEP measurement subsystem. The schematic and working procedure of the AO subsystem are described in detail elsewhere (Zhao et al., 2016).

In this AO subsystem, the lights from a beacon SLD (shown in Fig. 1) (λ = 795 nm, $\Delta\lambda$ = 18.8 nm) passed through a series of optical paths (L1, BS1, SM4-1, M4-2, M1, DM) and were finally imaged onto the retina. The backward scattered light from the eye fundus exited through the pupil, passed through the reverse optical path, and then was reflected onto a 16 × 16 Shack Hartmann wavefront sensor to measure the wavefront and the DM was used to correct ocular aberrations in real-time over a 6.0 mm pupil (Dai et al., 2015). In addition, defocus and astigmatism were corrected by means of a pair of rotating cylinders (RC) in combination with a Badal focus corrector (M3-2). The SLD using a near-infrared light can provide more comfortable viewing conditions and higher retinal reflectance. Thus, the AO working procedure did not interfere with the presentation of stimulus patterns during PR-VEP measurements.

In the PR-VEP measurement subsystem, the lights from the OLED (EMA-100100, eMagin, Inc., USA) black-and-white micro-display were imaged at infinity by an object lens L2. After being reflected by M5, the light travelled through the beam splitters BS2 and BS1 into the AO illumination path. Finally, it followed the illumination path into the eye. The stimuli patterns were generated by OpenGL3.3, and the video signal was input into a Bits# stimulus processor (Cambridge Research Systems Ltd., UK), which transferred the pattern stimulus to the OLED display and simultaneously sent a sync signal to the PR-VEP measurement system. The sync signal was used to trigger PR-VEP system acquisition synchronously with the stimulus presentation. The OLED with an effective size of 12 mm × 8 mm, a resolution of 800 × 600 pixels, and a maximum refresh rate of 75 Hz. Considering the anisoplanatism (Nowakowski, Sheehan, Neal, & Goncharov, 2012) of ocular aberration correction with AO, only the central 2° field of view of the display was used to present the stimuli. The PR-VEP acquisition circuit (Gao, Liu, & Cai, 2013) was developed by the University of Electronic Science and Technology of China, with a resolution of 16 bits and a sampling rate of 1000 Hz. The signal was amplified with a preamplifier and the bandpass was 1–30 Hz. The acquired PR-VEP data were stored in the computer for offline processing.

Table 1
Detailed information for all subjects.

Subject	Refractive error		Age/Eye	Sex
	OD	OS		
1	−0.75	−2.00–0.25 × 15°	22/OD	F
2	−1.25	−0.75	24/OS	F
3	−1.75–0.5 × 110°	−1.00–0.25 × 119°	22/OS	M
4	−2.75–0.5 × 8°	−2.75–1.00 × 2°	24/OD	M
5	−2.75–0.5 × 145°	−1.50	23/OS	M
6	−1.00–0.5 × 99°	−0.25–0.25 × 87°	25/OS	M
7	−3.25–150 × 8°	−1.75–2.00 × 14°	21/OS	M
8	−3.50	−3.50–0.25 × 139°	23/OD	F
9	−3.25–0.5 × 10°	−3.00	24/OD	F
10	−5.00–0.5 × 178°	−4.75–0.75 × 10°	32y/OD	M
11	−3.50–0.5 × 94°	−2.50–0.75 × 121°	26y/OD	M
12	−1.50–0.25 × 150°	0.25–0.25 × 19°	20y/OD	M

2.2. Subjects

Twelve healthy volunteers (four female and eight male) aged between 20 and 32 years participated in the study. Table 1 lists detailed information for all subjects. Each subject had normal corrected visual acuity with appropriate refraction. Each subject was treated with dilation of the pupil and paralysis of accommodation by administering 1% cyclopentolate. After 15 min of dark adaptation, the data were measured using the dominant eye. The study was approved by the Medical Ethics Committee at the Affiliated Ophthalmological Hospital, Chengdu University of Traditional Chinese Medicine. Informed consent was obtained from all subjects and the experimental procedures conformed to the tenets of the Declaration of Helsinki.

2.3. Procedures

To quantify the improvement of subjective visual performance with HOA correction, a contrast sensitivity function (CSF) was first measured in white light for the dominant eye of the 12 subjects, with and without HOA correction. The CSF was measured at spatial frequencies of 1, 2, 4, 8, 12, 16, and 24 cycles per degree (cpd) with a background luminance of 4.7 cd/m^2 in the pupil plane. The contrast of the stimuli was controlled through an adaptive staircase procedure. Three successive correct responses led to a contrast decrease of 10% of the previous value; one incorrect response brought a 10% increase. More details of the procedures can be found in Kang, Dai, and Zhang (2015).

The PR-VEP was recorded for the dominant eye of the 12 subjects with LOA or HOA correction (where LOA correction refers to correcting defocus and astigmatism, and HOA correction (Williams et al., 1997; Yang et al., 2018) to correcting the aberrations up to the eighth Zernike order). All the following expressions have the same meaning. The active electrode was positioned in the midline approximately 3 cm above the inion. The reference electrode was placed on the forehead, and the

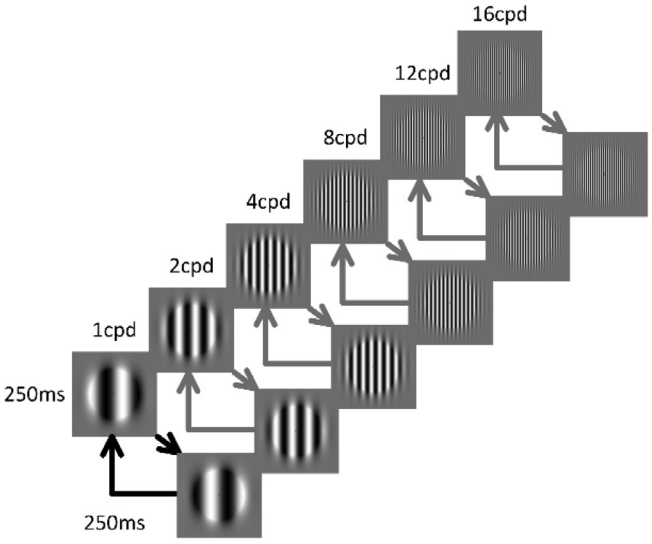

Fig. 2. Time sequence of the pattern stimulus displayed at each spatial frequency.

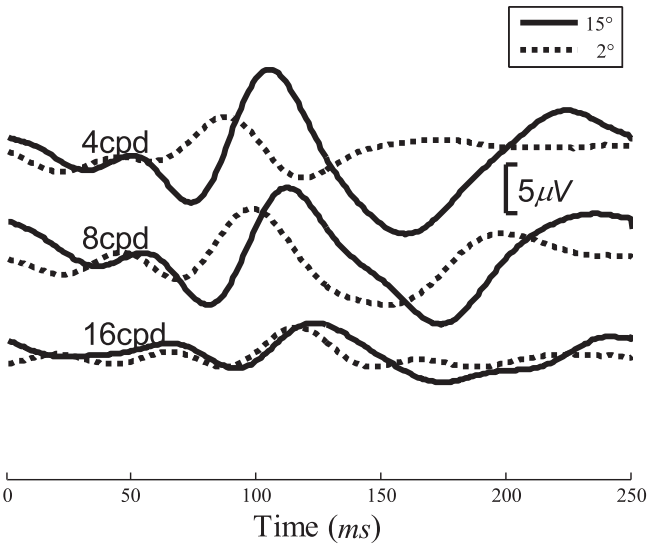

Fig. 3. Acquired PR-VEP waveforms of one subject under two field sizes; i.e., 15° and 2°, at 4, 8, and 16 cpd.

ground was attached to the earlobe mastoid. The electrodes were coated with a conductive paste (GT20, Wuhan Greentek Pty. Ltd, Wuhan, China) before being fixed to the corresponding position. The pattern stimulus was a vertically oriented 2°-field-of-view sinusoidal grating with a contrast of more than 95%, which was the same background luminance as in the CSF measurement, and spatial frequencies were 1, 2, 4, 8, 12, and 16 cpd. To minimize edge effects, a half-Gaussian ramp (Dai et al., 2015) was used to blend the stimuli into the background. The pattern stimulus was presented counter-phased at a frequency of 4 reverses per second (rps), and a small cross in the center of the screen was used as a fixation point. Fig. 2 shows the time sequence of the pattern stimulus displayed at each spatial frequency. PR-VEP acquisition was conducted in an electromagnetically shielded darkroom. The spatial frequencies of the pattern stimulus were presented randomly, and the PR-VEP at each spatial frequency was averaged from 100 pattern reversals and repeated three times to check the reproducibility of the waveform. The PR-VEP acquisition time at each spatial frequency was 25 s, followed by 10 s of rest time; the total experimental time was approximately 12 min. The latencies and amplitudes of N1, P1, and N2 of each PR-VEP waveform were extracted and compared to assess the effects of HOAs on PR-VEP.

3. Results

3.1. PR-VEPs with a 2° field size

The International Society for Clinical Electrophysiology of Vision (ISCEV) recommends that the field size should be larger than 15° for PR-VEP testing (Odom et al., 2010). In the AO PR-VEP measurement system, the field size of the stimulus was limited to 2°, which was far less than that recommended by ISCEV. Fig. 3 shows the acquired PR-VEP waveforms of one subject under two field sizes of 15° and 2° at spatial frequencies of 4, 8, and 16 cpd. From the results, the VEP waveform under a 2° field size also consisted of a negative N1 peak, a positive P1 peak, and a second negative N2 peak, which was similar to the results for a less than 15° field size. Upon comparison with a large 15° field size, the amplitudes and latencies were attenuated and shortened at all spatial frequencies, and the latency variation decreased with increasing spatial frequency under the 2° field size. The PR-VEP was too weak to be recorded at a spatial frequency of 24 cpd due to signal attenuation under a 2° field size.

3.2. Test-retest repeatability

Under the small 2° field size, the PR-VEP measurement at each spatial frequency was repeated three times to check the reproducibility of the acquired waveform for each subject. (American Clinical Neurophysiology Society Guideline, 2016) Fig. 4 shows the testing results for one subject who showed good repeatability. If the results of the three repeated measurements were not reproducible, the subject was retested.

Fig. 5 shows the test repeatability for one subject over three days. From the results, all the data of PR-VEP components were within the 95% confidence interval, and the test results had good repeatability.

3.3. Contrast sensitivity function

Fig. 6 shows the average contrast sensitivity function results for the 12 subjects. HOA correction improved contrast sensitivity at all spatial frequencies, with improvement by a factor of 1.28, 1.33, 1.16, 1.21, 1.18, 1.23, and 1.41 at 1, 2, 4, 8, 12, 16, and 24 cpd, respectively. As a result, the visual benefit was generally larger at higher spatial

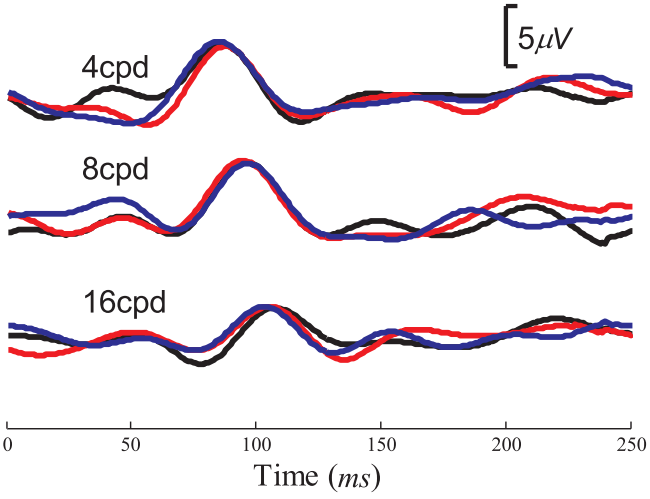

Fig. 4. PR-VEP waveform measured with the AO PR-VEP system.

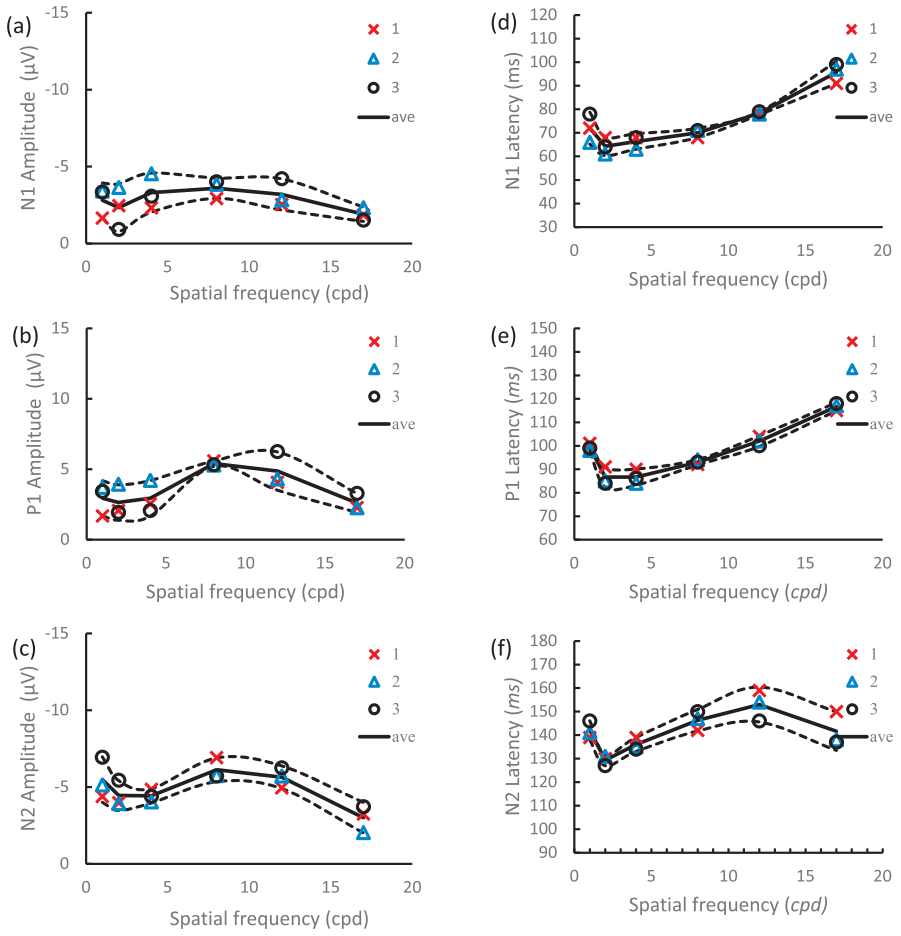

Fig. 5. Test-retest variations of the latencies and amplitudes of N1, P1, and N2 of each PR-VEP waveform from one subject over three days.

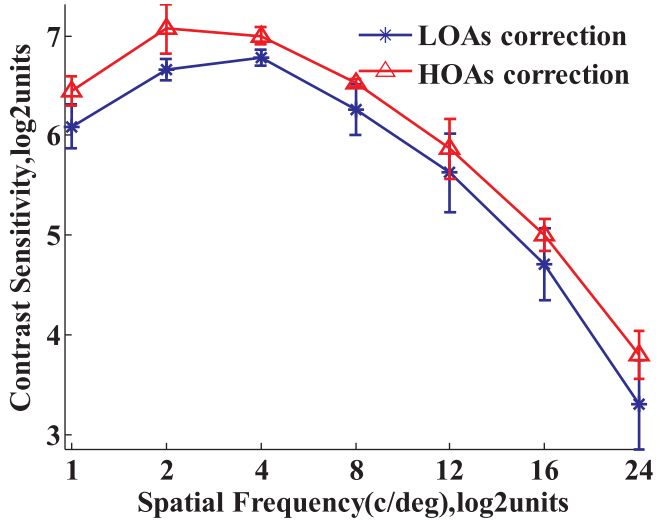

Fig. 6. Contrast sensitivity function averaged across the 12 subjects. The blue asterisks represent contrast sensitivity measured with LOA correction; red triangles represent contrast sensitivity measured with AO correction of HOAs. Error bars indicate standard deviations.

frequencies (Kang et al., 2015). The data were assessed with a paired *t*-test, and the results revealed that the contrast sensitivity improvement was statistically significant for all spatial frequencies ($p < 0.05$), indicating that the HOA correction was effective.

3.4. PR-VEP waveforms before and after HOA correction

The residual LOAs after static compensation by the RC in combination with the Badal were corrected by AO in real time. Fig. 7(a) shows the corresponding root-mean-square (RMS) curves of total aberrations and HOA curves with time for one subject. Data during eye blinks had already been removed. After LOA correction with the AO system, the average residual total RMS, except tip and tilt, converged to a value of approximately 0.329 μm. The residual LOAs were almost completely corrected by the AO system, as evidenced from component analysis of residual aberrations. Upon LOA correction, the PR-VEP waveforms were acquired for all 12 subjects with spatial frequency randomly changed from 1 to 16 cpd. The PR-VEP waveforms from one subject at each spatial frequency are shown in Fig. 7(b). The waveforms are shown after baseline correction as the amplitude was 0 μV at the start time.

To evaluate the effects of HOAs on PR-VEP, HOA correction that corrected the aberration up to the eighth Zernike order was used for comparison. Fig. 8(a) shows the time course of the RMS curves of total aberrations and the HOAs of one subject. The average RMS curves of residual aberrations converged rapidly from 0.329 μm to a small value of approximately 0.041 μm after HOA correction (t = 92 s). Upon HOA correction, the PR-VEP waveforms were acquired for all subjects with spatial frequency randomly changed from 1 to 16 cpd. The PR-VEP waveforms from one subject at each spatial frequency are shown in Fig. 8(b).

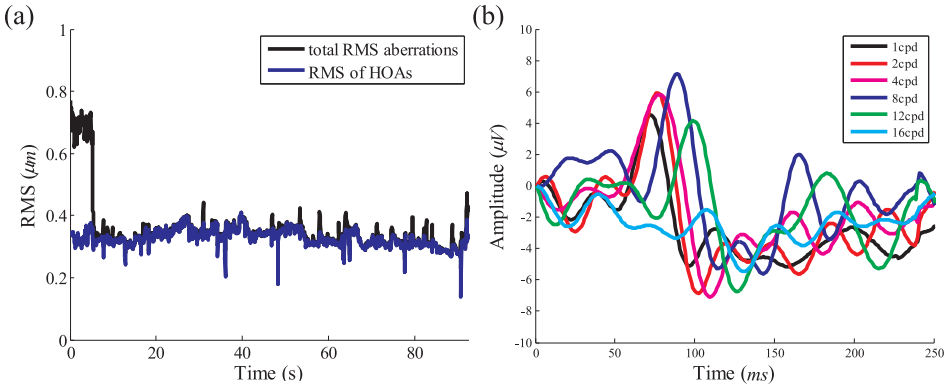

Fig. 7. (a) RMS curve with time in the process of recording, and (b) corresponding averaged PR-VEP waveforms with LOA correction with the AO system.

3.5. Effects of HOAs on each component of the PR-VEP

To assess the effects of HOAs on PR-VEP, we compared the data acquired from HOAs that was retained and corrected. Fig. 9 shows the averaged wavefront RMS of all subjects with LOA and HOA correction. Obviously, the RMS across all subjects decreased after HOA correction to an average of 20.7% of the RMS with LOA correction. These optical benefits contributed to the improvements in visual performance, such as CSF and PR-VEP.

Fig. 10(a)– (c) show the averaged N1, P1, and P2 amplitudes at each spatial frequency with LOA and HOA correction. Compared with LOA correction, the P1 and N2 amplitudes increased by different levels at all spatial frequencies with HOA correction. The N1 amplitudes also increased at all spatial frequencies, except at 12 and 16 cpd. The increased ratios of the HOA correction amplitude to that of the LOA correction are shown in Table 2. Relative to LOA correction, the increased N1 ratio was approximately 15%–59% at each spatial frequency after HOA correction, and the maximal value was reached at 4 cpd. The increased P1 ratio was approximately 9%–36% with HOA correction, and the maximal ratio was reached at 1 and 16 cpd. The increased N2 ratio was approximately 3%–32%, and the maximal point was reached at 16 cpd. The data were referred to a paired *t*-test for statistical analysis, and the increased P1 (except 2 cpd) and N2 (at 12, 16 cpd) ratios were statistically significant ($p < 0.05$).

Fig. 10(d)–(f) show the averaged latency at each spatial frequency between LOA and HOA correction. Compared with the LOA correction, the effect of HOA correction exhibited no regularity in the changes of N1, P1, and N2 latencies. The N1 latencies were shortened from approximately 4–0 ms from 1 to 8 cpd and prolonged by 1–4 ms from 12 to 16 cpd with HOA correction. The P1 latencies at each spatial frequency were prolonged by 0–6 ms, except at 2 cpd they were shortened by 1 ms and the N2 latencies were prolonged by approximately 0–3 ms from 8 to 16 cpd and shortened by 3 and 4 ms at 2 and 4 cpd, respectively, with HOA correction. The data were analyzed with a paired *t*-test for statistical analysis, and all were not statistically significant

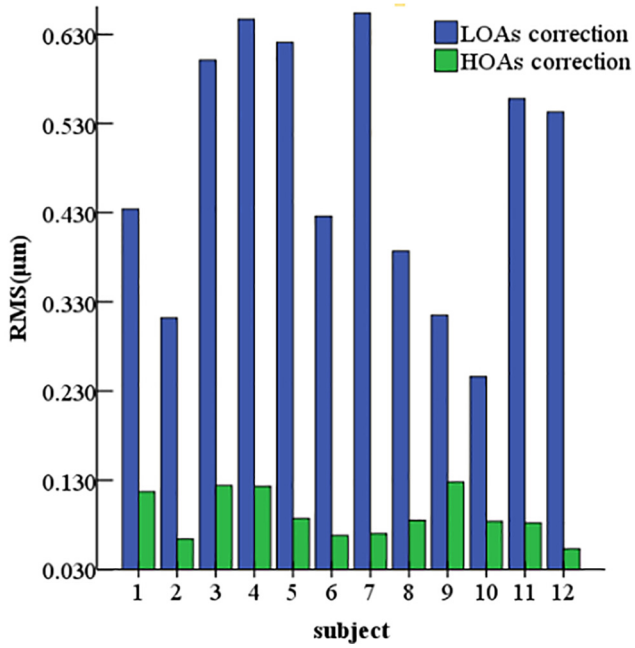

Fig. 9. Wavefront RMS of each subject with no HOA correction and HOA correction.

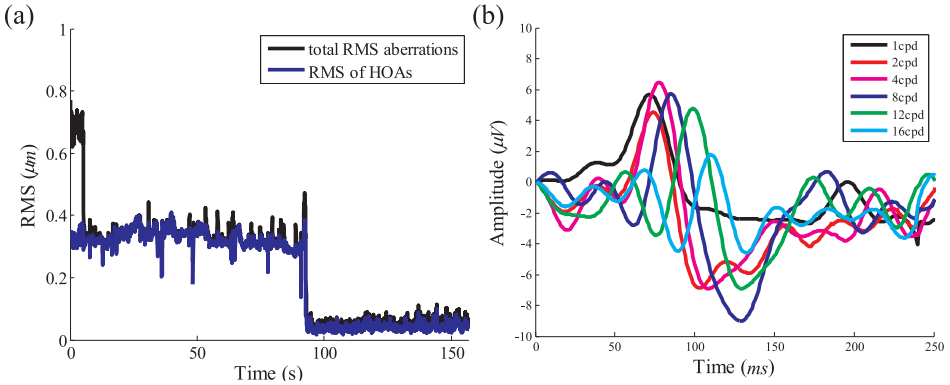

Fig. 8. (a) Time course of RMS curves of total aberrations and HOAs with HOA correction for one subject. HOA correction is initiated at t = 92 s. (b) PR-VEP waveform for one subject at each spatial frequency with HOA correction.

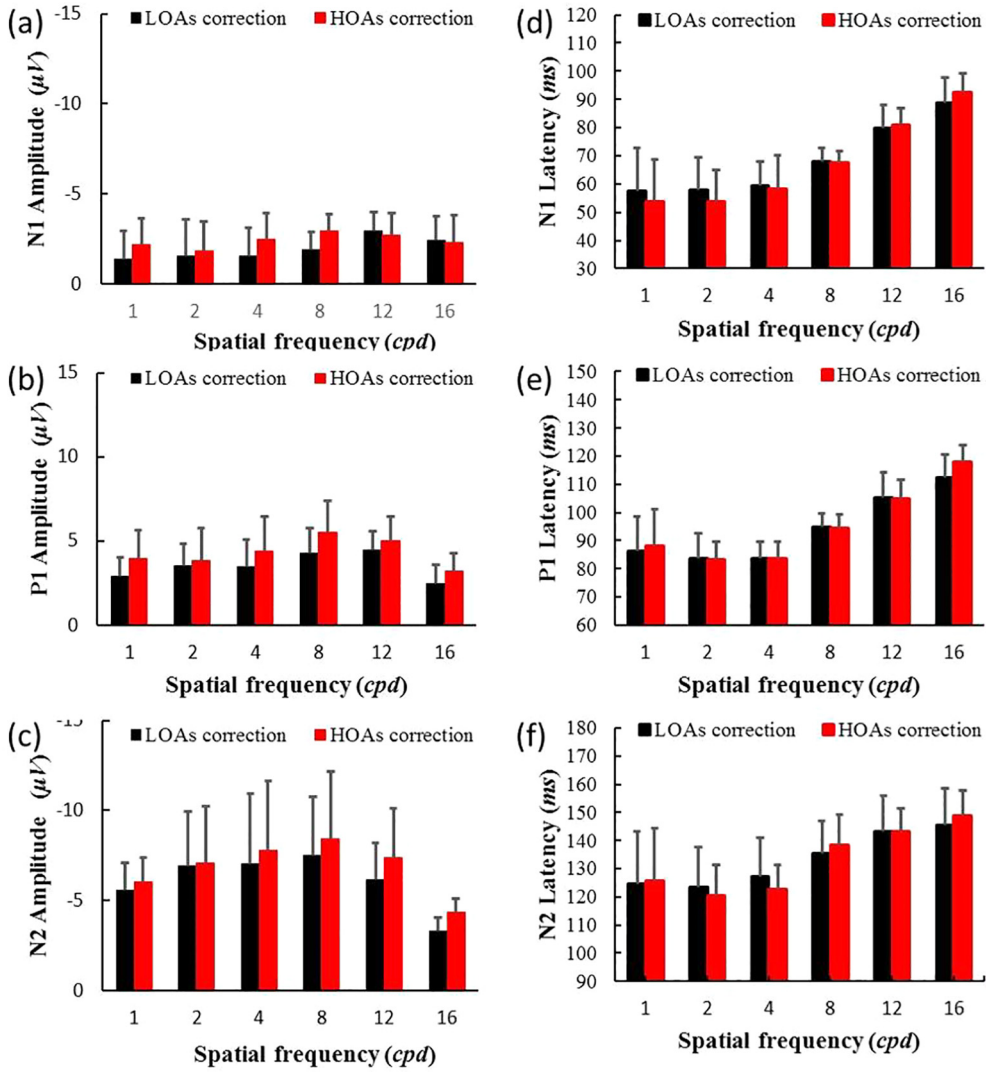

Fig. 10. (a)–(c) Averaged amplitudes and (d)–(f) latencies of VEPs between LOA and HOA correction from all subjects. Plots are shown with the mean and standard deviation.

Table 2
Increased ratio of amplitudes and variation of latency for each component with LOA and HOA correction at each testing spatial frequency.

Spatial frequency (cpd)	1	2	4	8	12	16
N1 amplitude increased ratio (%)	59	15	63	53*	−7	−5
P1 amplitude increased ratio (%)	36*	9	27*	29*	13*	31*
N2 amplitude increased ratio (%)	8	3	12	12	21*	32*
N1 latency variation (ms)	−4	−4	−1	0	1	4
P1 latency variation (ms)	2	−1	0	0	0	6
N2 latency variation (ms)	1	−3	−4	3	0	3

* $P < 0.05$ for the LOA correction versus the HOA correction.

($p > 0.05$).

From these comparisons between HOAs that were retained and corrected, it can be concluded that the ocular aberrations, especially HOAs, differently influenced NPN amplitudes and latencies. First, the correction improved retinal image quality and excited more neurons as more visual cells received a clearer image. Second, it increased the number of excited nerve fibers that reached the visual cortex and increased the NPN amplitudes. For NPN latencies, after HOA correction it did not change the spatial frequencies and field size. As a result, the change in NPN latency was not obvious. From this point of view, the NPN amplitude was equivalent to the subjective perception or the retinal image quality. According to this equivalent principle, PV-VEP could be used to objectively measure refractive power (Regan, 1973) and to objectively evaluate visual performance.

In addition, N1 is an absolute value while P1 and N2 are relative values as we defined them. Accordingly N1 is more affected by factors such as a spontaneous EEG signal, fixation, emotion, mental activities and so on, even though the VEP waveforms were corrected to the baseline.

4. Discussion

The VEP waveform is a sensitive indicator of a variety of pathological conditions, such as amblyopia, glaucoma, optic neuritis, multiple sclerosis, and other visual pathway dysfunctions originating from the receptor cells to the visual cortex. However, many non-pathological factors can have a serious impact on VEP testing results. Among these factors, ocular aberration is one of the most important because it directly degrades the retinal image quality of the pattern stimulus. Traditional refractive error correction can only compensate for LOAs. In this article, the effects of HOAs on PR-VEP have been studied for the first time to the best of our knowledge. From these preliminary experimental results, the increased P1 (except 2 cpd) and N2 (at 12, 16 cpd) with HOA correction were statistically significant, although

there was no statistically significant effect with the other components of the PR-VEP waveform. When we make use of the P1 and N2 amplitudes for visual pathway disease diagnosis, the existence of HOAs may lead to misdiagnosis.

Compared to the CSF, the improvements in P1 amplitude did not increase steadily with spatial frequency after HOA correction. The biggest improvement in P1 amplitude was at 1 cpd, followed by 16 cpd and 8 cpd, while the biggest improvement in CSF was at 24 cpd, followed by 1 cpd and 2 cpd. However, it is well known that the higher the spatial frequency, the larger benefit of HOA correction on visual performance. Discrepant optical improvements in visual performance have been found in other studies (De Gracia, Marcos, Mathur, & Atchison, 2011). The reported neural limits or neural insensitivity, and even psychophysical factors and imprecise AO corrections, may be attributable to these discrepancies.

In our results, the averaged P1 amplitudes ranged from 2.47 to 4.45 μV across all spatial frequencies, and the largest amplitude was at 12 cpd. The averaged P1 latencies ranged from 83.7 to 112.4 ms, with the longest at 16 cpd. Compared to the normal P1 amplitudes and latencies in Gundogan et al. (2010), the P1 amplitudes were obviously decreased and the P1 latencies were slightly shortened with the AO PR-VEP measurement system. Furthermore, all amplitudes at 1 cpd were beyond the normal range, while only two (2/12) at 2 cpd and four (4/12) at 4 cpd were in the normal range. The differences in amplitudes could be the result of different field sizes. Therefore, standard databases for the AO PR-VEP measurements need to be established as different laboratories use different stimulus conditions clinically.

Considering the anisoplanatism of ocular aberration correction with an AO system, only a 2° field size was used in this study, which was small relative to the traditional greater than 15° field size recommended by ISCEV. The limited field size reduced the amplitude of the PR-VEP waveform, and therefore an acquisition circuit with high sensitivity and a higher number of sweeps to be averaged to improve the SNR is required. However, while the subjective CSF at a high spatial frequency; i.e., 24 cpd, can be measured, the objective VEP cannot be recorded due to the reduced amplitude of the PR-VEP waveform and limited SNR. Regardless, similar to the traditional PR-VEP waveform, the amplitude-tuning functions of P1 and N2 with a 2° field size showed an obvious inverted-U shape (Zhou et al., 2007). Where the largest averaged P1 amplitude was at 12 cpd, it was higher than the reported 8–25 arc (Siegfried, 1975). The difference was related to stimulus conditions such as the range of spatial frequencies and field size.

From this point of view, the smaller the size of the field, the better the ability to position a defect in the visual field. Comparing the field sizes of 15 and 2°, there were distinctly different attenuations in amplitude for each spatial frequency (such as 4 and 16 cpd). The PR-VEPs at low spatial frequencies were mainly from the perifoveal area (large field size), while the parafoveal area (narrow field size) was the main source of PR-VEP at high spatial frequencies. Thus, the AO PR-VEP measurement system was better for high spatial frequencies (e.g. 16 and 24 cpd). As retinal image quality was improved and more neurons were excited when using the AO system to bypass the optical limit, especially for HOAs, it provides an objective and quantitative tool for accurate assessment of visual performance with VEP measurements. From the perspective of VEPs, it could objectively explore the extent to which the visual system exploits the increase in optical quality.

In the present study, 12 healthy eyes with low HOAs relative to a diseased eye (Zhao et al., 2016) were tested. The relatively small amount of HOAs (approximately 0.3 μm RMS for all subjects) significantly affected only the P1 and N2 amplitudes. With the increasing HOAs of diseased eyes, such as keratoconus and amblyopia, whether other components of the VEP are affected requires further study. Beyond this, the effect of individual Zernike aberrations on PR-VEP testing is another issue worthy of study.

5. Conclusion

In this study, we investigated the effect of high-order aberrations (HOAs) on the PR-VEPs. PR-VEP measurements of 12 subjects with normal vision were performed with HOAs either retained or corrected by the AO system. After HOA correction, the amplitude of the first positive P1 wave and the second negative N2 wave were raised by different ratios with statistical significance at spatial frequencies ranging from 1 to 16 cpd. No statistically significant influence was found on other components of the PR-VEP waveform. These results confirm the contributions of the HOAs to the alterations of the PR-VEP waveform and suggest that HOAs should be corrected to realize accurate PR-VEP testing.

Acknowledgments

This work was supported by National Natural Science Foundation of China (61378064) and National High Technology Research and Development Program of China (2015AA020510).

The authors would like to thank Professor Wenhan Jiang for critical comments and thoughtful suggestions. We also thank all subjects for their positive support in this work.

References

Abdullah, S. N., Aldahlawi, N., Rosli, Y., Vaegan, Boon, M. Y., & Maddess, T. (2012). Effect of contrast, stimulus density, and viewing distance on multifocal steady-state visual evoked potentials (MSVs). *Investigative Ophthalmology & Visual Science, 53*(9), 5527–5535.

Abe, H., Hasegawa, S., & Iwata, K. (1987). Contrast sensitivity and pattern visual evoked potential in patients with glaucoma. *Documenta Ophthalmologica, 65*(1), 65–70.

American Clinical Neurophysiology Society Guideline 9 B: Guidelines on Visual evoked potentials (2006). Journal of Clinical Neurophysiology 23(2) 138–156.

Andreassi, J. L., Mayzner, M. S., Beyda, D. R., & Davidovics, S. (1970). Effects of induced muscle tension upon the visual evoked potential and motor potential. *Psychonomic Science, 20*(4), 245–247.

Bach, M., & Mathieu, M. (2004). Different effect of dioptric defocus vs. light scatter on the Pattern Electroretinogram (PERG). *Documenta Ophthalmologica, 108*(1), 99–106.

Bartel, P. R., & Vos, A. (1994). Induced refractive errors and pattern electroretinograms and pattern visual evoked potentials: Implications for clinical assessments. *Electroencephalography and Clinical Neurophysiology, 92*(1), 78–81.

Collins, D. W. K., Carroll, W. M., Black, J. L., & Walsh, M. (1979). Effect of refractive error on the visual evoked response. *British Medical Journal, 1*(6158), 231–232.

Dai, Y., Zhao, L., Xiao, F., Zhao, H., Bao, H., & Zhou, H. (2015). Adaptive optics vision simulation and perceptual learning system based on 35-element bimorph deformable mirror. *Applied Optics, 54*(5), 979–985.

De Gracia, P., Marcos, S., Mathur, A., & Atchison, D. A. (2011). Contrast sensitivity benefit of adaptive optics correction of ocular aberrations. *Journal of Vision, 11*(12).

Dion, L., Muckle, G., Bastien, C., Jacobson, S. W., Jacobson, J. L., & Saint-Amour, D. (2013). Sex differences in visual evoked potentials in school-age children: What is the evidence beyond the checkerboard? *International Journal of Psychophysiology, 88*(2), 136–142.

Gao, D., Liu, T., Cai, J., et al. (2013) An EEG acquisition system with dynamic DC suppression. World congress on Medical Physics and Biomedical Engineering May 26-31, 2012, Beijing, China, IFMBE Proceedings 39, pp. 1483–1486.

Gundogan, F. C., Mutlu, F. M., Altinsoy, H. I., Tas, A., Oz, O., & Sobaci, G. (2010). Pattern visual evoked potentials in the assessment of objective visual acuity in amblyopic children. *International Ophthalmology, 30*(4), 377–383.

Gundogan, F. C., Mutlu, F. M., Ibrahim, A. H., Tas, A., Oz, O., & Sobaci, G. (2010). Pattern visual evoked potentials in the assessment of objective visual acuity in amblyopic children. *International Ophthalmology, 30*, 377–383.

Halliday, A. M. (1982). *Text book of Evoked potential in clinical testing.* New York: Churchill Livingstone90–91.

Halliday, A. M., McDonald, W. I., & Mushin, J. (1972). Delayed visual evoked responses in optic neuritis. *Lancet, 299*(7758), 982–985.

Harter, M. R., & White, C. T. (1968). Effects of contour sharpness and check-size on visually evoked cortical potentials. *Vision Research, 8*(6), 701–711.

Hoeppner, T., & Lolas, F. (1978). Visual evoked responses and visual symptoms in multiple sclerosis. *Journal of Neurology Neurosurgery & Psychiatry, 41*(6), 493–498.

Kang, Jian, Dai, Yun, & Zhang, Yudong (2015). Temporal integration property of stereopsis after higher-order aberration correction. *Biomedical Optics Express, 6*(11), 4472–4482.

Kothari, R., Bokariya, P., Singh, S., Narang, P., & Singh, R. (2014). Refractive errors and their effects on visual evoked potentials. *Journal of Clinical Ophthalmology & Research, 2*(1), 3–6.

Liang, J., Grimm, B., Goelz, S., & Bille, J. F. (1994). Objective measurement of wave aberrations of the human eye with use of a Hartmann-Shack wave-front sensor. *Journal of the Optical Society of America A, 11*(7), 1949–1957.

Mezer, E., Bahir, Y., Leibu, R., & Perlman, I. (2004). Effect of defocusing and of distracted attention upon recordings of the visual evoked potential. *Documenta Ophthalmologica, 109*(3), 229–238.

Nowakowski, Maciej, Sheehan, Matthew, Neal, Daniel, & Goncharov, Alexander V. (2012). Investigation of the isoplanatic patch and wavefront aberration along the pupillary axis compared to the line of sight in the eye. *Biomedical Optics Express, 3*(2), 240–258.

Odom, J. V., Bach, M., Brigell, M., Holder, G. E., McCulloch, D. L., & Tormene, A. P. (2010). ISCEV standard for clinical visual evoked potentials (2009 update). *Documenta Ophthalmologica, 120*(1), 111–119.

Regan, D. (1973). Rapid objective refraction using evoked brain potentials. *Investigative Ophthalmology, 12*(9), 669–679.

Roorda, A. (2011). Adaptive optics for studying visual function: A comprehensive review. *Journal of Vision, 11*(7), 74–76.

Siegfried, John B. (1975). The effects of checkerboard pattern check size on the VEP. *Bulletin of the Psychonomic Society, 6*(3), 306–308.

Stockard, J. J., Hughes, J. F., & Sharbrough, F. W. (1979). Visually evoked potentials to electronic pattern reversal: Latency variations with gender, age and technical factors. *American Journal of Eeg Technology, 19*(4), 171–204.

Wenner, Y., Heinrich, S. P., Beisse, C., Fuchs, A., & Bach, M. (2014). Visual evoked potential-based acuity assessment: Overestimation in amblyopia. *Documenta Ophthalmologica, 128*(3), 191–200.

Williams, D. R., Miller, D. T., & Liang, J. (1997). Supernormal vision and high-resolution retinal imaging through adaptive optics. *Journal of the Optical Society of America A Optics Image Science & Vision, 14*(11), 2884.

Yang, Y., Zhao, J., Zhao, H., Xiao, F., Xie, J., Liu, T., et al. (2018). Objective visual performance evaluation with visual evoked potential measurements based on an adaptive optics system. *Chinese Optics Letters, 16*(5), 053301.

Zhao, J., Xiao, F., Kang, J., Zhao, H., Dai, Y., & Zhang, Y. (2016). Quantifying intraocular scatter with near diffraction limited double-pass point spread function. *Biomedical Optics Express, 7*(11), 4595–4604.

Zhao, J., Xiao, F., Kang, J., Zhao, H., Dai, Y., & Zhang, Y. (2016). Statistical analysis of ocular monochromatic aberrations in Chinese population for adaptive optics ophthalmoscope design. *Journal of Innovation in Optical Health Science, 10*(1), 1650038.

Zhou, P., Zhao, M., Li, X., Hu, X., Wu, X., Niu, L., et al. (2007). A new method for extrapolating the sweep pattern visual evoked potential acuity. *Documenta Ophthalmologica, 117*(2), 85–91.